Clim. Past Discuss., 8, 3205–3249, 2012
www.clim-past-discuss.net/8/3205/2012/
doi:10.5194/cpd-8-3205-2012

Climate of the Past Discussions

Multidisciplinary distinction of mass-movement and flood-induced deposits in lacustrine environments: implications for Holocene palaeohydrology and natural hazards (Lake Ledro, Southern Alps, Italy)

A. Simonneau[1], E. Chapron[1], B. Vannière[2], S. B. Wirth[3], A. Gilli[3], C. Di Giovanni[1], F. S. Anselmetti[4,*], M. Desmet[1,5], and M. Magny[2]

[1]ISTO, UMR7327, CNRS; Univ. Orléans; BRGM, 1A rue de la Férollerie, 45071 Orléans Cedex 2, France
[2]Laboratoire de Chrono-Environnement, UMR6249, CNRS; UFR des Sciences et Techniques, 16 route de Gray, 25030 Besançon, France
[3]Geological Institute, ETH Zurich, Sonneggstrasse 5, 8092 Zurich, Switzerland
[4]Eawag, Department of Surface Waters, Überlandstrasse 133, 8600 Dübendorf, Switzerland

[5]GéoHydrosystème COntinentaux, E.A. 6293 GéHCO, Université F. Rabelais de Tours, Département Géosciences-environnement, Faculté des Sciences et Techniques, Parc de Grandmont, 37200 Tours, France
[*]current address: Institute of Geological Sciences, University of Bern, Baltzerstrasse 1–3, 3012 Bern, Switzerland

Received: 19 July 2012 – Accepted: 24 July 2012 – Published: 3 August 2012

Correspondence to: A. Simonneau (anaelle.simonneau@univ-orleans.fr)

Published by Copernicus Publications on behalf of the European Geosciences Union.

Abstract

High-resolution seismic profiles and sediment cores from Lake Ledro combined with soil and river-bed samples from the lake's catchment area are used to assess the recurrence of natural hazards (earthquakes and flood events) in the southern Italian Alps during the Holocene. Two well-developed deltas and a flat central basin are identified on seismic profiles in Lake Ledro. Lake sediments are finely laminated in the basin since 9000 cal. yr BP and frequently interrupted by two types of sedimentary events: light-coloured massive layers and dark-coloured graded beds. Optical analysis (quantitative organic petrography) of the organic matter occurring in soils, river beds and lacustrine samples together with lake-sediment bulk density and grain-size analysis illustrate that light-coloured layers consist of a mixture of lacustrine sediments and mainly contain algal particles similar to the ones observed in background sediments. Light-coloured layers thicker than 1.5 cm in the main basin of Lake Ledro are dense and synchronous to numerous coeval mass-wasting deposits remoulding the slopes of the basin. They are interpreted as subaquatic mass movements triggered by historical and pre-historical regional earthquakes dated to 2005 AD, 1891 AD, 1045 AD and 1260, 2545, 2595, 3350, 3815, 4740, 7190, 9185 and 11495 cal. yr BP. Dark-coloured sedimentary event are dense and develop high-amplitude reflections in front of the deltas and in the deep central basin. These beds are mainly made of terrestrial organic matter (soils and ligno-cellulosic debris) and are interpreted as resulting from intense hyperpycnal flood events. Mapping and quantifying the amount of soil material accumulated in the Holocene hyperpycnal flood deposits of the sequence and applying the De Ploey erosion model allow estimating that the equivalent soil thickness eroded over the catchment area reached up to 4 mm during the largest Holocene flood events. Such significant soil erosion is interpreted as resulting from the combination of heavy rainfall and snowmelt. The recurrence of flash-flood events during the Holocene was however not high enough to affect pedogenesis processes and highlight several wet regional periods during the Holocene. The Holocene period is divided into four

phases of environmental evolution. Over the first half of the Holocene, a progressive stabilization of the soils present through the catchment of Lake Ledro was associated with a progressive reforestation of the area and only interrupted during the wetter 8.2 event when the soil destabilization was particularly important. Lower soil erosion was recorded during the Mid-Holocene climatic optimum (8000–4200 cal. yr BP) and associated with higher algal production. Between 4200 and 3100 cal. yr BP, both wetter climate and human activities within the drainage basin drastically increased soil erosion rates. Finally, from 3100 cal. yr BP to the present-day, results suggest increasing and changing human land-use.

1 Introduction

Climate variability and seismicity represent serious natural concerns to modern societies in the Alps (e.g. Beniston et al., 2007). Actual climate models project that future climate warming in Central Europe will bring more frequent extreme events and especially heavy precipitations and floods (Buma and Dehn, 1998; Christensen and Christensen, 2003; Beniston et al., 2007; Stewart et al., 2011). Flood hazards vary as a function of the hydroclimatic regime, position within the drainage basin and human interaction in the catchment (Wohl, 2000). Changes in the hydrological balance influence therefore the hydrological regime of the slopes and govern the type, rate and occurrence of natural extreme floods (Knox, 2000), associated soil erosion (De Ploey et al., 1995; Cerdà, 1998; Raclot and Albergel, 2006) and can affect human activities and societies especially in mountainous environments (Dearing, 2006; Dearing et al., 2006).

The Southern Alps in Italy are sensitive to natural hazards such as earthquakes and flash-floods (Tropeano and Turconi, 2004; Barredo, 2007; Marchi et al., 2010; Lauterbach et al., 2012). Former studies suggested that precipitation regimes in this part of the Alps may have been affected by Atlantic influences at millennial and multi-centennial time scales (Magny et al., 2009, 2012). Over the last decade, different

authors have also shown that lake sediments represent valuable archives to reconstruct past river discharges (Chapron et al., 2005; Bøe et al., 2006; Debret et al., 2010; Stewart et al., 2011; Wirth et al., 2011; Gilli et al., 2012) and past seismic events (Chapron et al., 1999; Schnellmann et al., 2002; Fanetti et al., 2008; Lauterbach et al., 2012).

In this paper, drainage basin descriptions of slope and soils are combined with seismic profiles and sedimentological analysis of lacustrine cores retrieved from peri-Alpine Lake Ledro (Italy, 45° N). On the basis of the Holocene chronology presented in Vannière et al. (this issue) established on sediment cores, our results propose a new organic geochemistry approach to distinguish the sources of exceptional deposits attributed to natural hazards such as earthquakes or flash-floods. This allows the reconstruction of past regional seismicity and wet regional periods during the Holocene. Finally, our paleoenvironmental reconstructions highlight the potential influence of recurrent natural hazards on the evolution of lake-dwelling at the shore of Lake Ledro during the Middle Bronze Age.

2 Study area

The drainage basin of Lake Ledro covers 111 km^2, culminates at 2254 m above sea level (m a.s.l.) and is today influenced by a subcontinental climate characterized by mean total annual precipitations of 900 mm, mean annual temperature of 8 °C and significant snowfalls in winter above 1500 m a.s.l. (Beug, 1964). Recent river corrections have been installed in the Massangla River (west of Lake Ledro) and the Pur River (south of Lake Ledro) in order to reduce the effects of flood events. Indeed, these two temporary torrential tributaries of Lake Ledro and their drainage network create canyons or gullying on steep slopes, transport decimetric blocks and export the fine fraction to the lacustrine basin (Fig. 1). Lake Ledro (45°52′ N/10°45′ E) is a small basin (3.7 km^2, 2.6 km long, 1.3 km wide, 46 m deep) of glacial origin blocked by a frontal moraine in the east at 653 m a.s.l., where the Ponale River forms the outlet of the lake

draining into Lake Garda located at 65 m a.s.l. Since 1929 AD, the level of Lake Ledro has been regulated for hydroelectricity production between lakes Ledro and Garda.

The bedrock of the drainage basin of Lake Ledro is composed of Mesozoic rocks with Triassic dolomite and Jurassic and Cretaceous limestones. The steep slopes (> 30 %, 50 km^2, yellow areas in Fig. 1b) are formed by Quaternary glacial and fluvial deposits (Bollettinari et al., 2005) and are covered by forest and open landscape (> 2000 m a.s.l.). In contrast, two flat valleys (0–5 %, hatched red areas in Fig. 1b) correspond to the paleolake Ledro maximal extension after glacier retreat and to the present-day alluvial plains of the Massangla and Pur rivers. These alluvial plains and the lake shorelines are associated with agricultural areas and human settlements since at least the Bronze Age, corresponding at Lake Ledro to a period of development of lake-dwelling which declined around 3100 cal. yr BP (Magny et al., 2009). In addition, this part of the Southern Alps was affected by five strong regional earthquakes over the last millennia (Guidoboni et al., 2007, Fig. 1a, Table 1).

3 Methods

The sedimentary infill of the lake was imaged in fall 2007 by high-resolution seismic profiling (Fig. 2a). A 3.5 kHz pinger system navigated with a GPS was employed from an inflatable boat. A dense grid of profiles enable us to establish the seismic stratigraphy of the lacustrine infill and allowed the determination of two coring sites: LL082 (14.6 m core length) in the central deepest basin (water depth: 46 m) and LL081 (9.9 m core length) in the eastern part of the central basin (water depth: 45 m) (Fig. 2c). These two cores were retrieved in areas lacking massive reworked material (Fig. 2) using the UWITEC piston corer from a platform. Continuous composite sections were defined using two parallel cores at each site. The stratigraphic correlation between the two coring sites is supported by the identification of characteristic lithological layers and the seismic stratigraphy. Initial core analysis of LL082 and LL081 included gamma-ray attenuation density measured with a GEOTEK multi-sensor core logger (sampling

interval: 0.5 cm), macroscopic core description and digital photographs. Laser diffraction grain-size measurements were performed using a Malvern Mastersizer 2000. Age-depth models of lacustrine cores are based on gamma-spectroscopic radionuclide measurements (^{137}Cs, ^{210}Pb) on core LL082 and 17 AMS radiocarbon dates (6 on LL082 and 11 on LL081, Fig. 3a) that are reported in Vannière et al. (this issue).

In July 2011, 11 pedological profiles and 6 river beds were sampled within the watershed (coloured circles in Fig. 1b). They were selected at different altitudes and under various vegetation covers in order to be representative of (i) high-altitude thin soils composed of lithic and rendzic Leptosols (62 % of the catchment area), (ii) well-developed soils composed of Cambisols (21 % of the catchment area) and (iii) alluvial soils divided into colluvic Regosols and Fluvisols (17 % of the catchment area).

Organic geochemistry of lake sediments and catchment area samples was measured by Rock-Eval pyrolysis (RE) and quantitative organic petrography (QOP). RE is used to characterize the organic content of natural samples by thermal cracking (Espitalié et al., 1985; Behar et al., 2001). RE parameters as the Total Organic Carbon (TOC, %), the S2 (expressed in mgHC) and the thermal maturity (Tpeak, °C) measurements can be used to characterize soil organic matter (Di Giovanni et al., 1998; Sebag et al. 2005; Copard et al., 2006) and to discriminate between an aquatic or terrestrial origin of the organic matter into lacustrine environments (Talbot and Livingstone, 1989; Millet et al., 2007). S2 represents the total amount of hydrocarbon that escapes from the sample during the thermal cracking (Ariztegui et al., 2001). The regression lines (slopes) of the diagram S2 *versus* TOC determine constant values of the Hydrogen Index (HI, expressed in mgHC g^{-1}TOC) since HI = (S2 × 100)/TOC (Behar et al., 2001). Classically, two particular slopes, corresponding to HI equals to 750 and 300 mgHC g^{-1}TOC, respectively, are represented in the S2 *versus* TOC diagrams in order to identify the chemical quality or the origin of the organic compounds (Ariztegui et al., 2001). Values of HI inferior to 300 mgHC g^{-1}TOC can point towards organic matter oxidation in the sediment or a contribution of terrestrial material (Ramanampisoa and Disnar, 1994; Disnar et al., 2003; Calvert, 2004; Jacob et al., 2004; Millet et al., 2007).

Inversely, HI values superior to 300 mgHC g^{-1}TOC suggests well preserved organic matter in the sediment or higher contributions of lacustrine algal particles which the specific pole is represented by HI values superior to 750 mgHC g^{-1}TOC (Talbot and Livingstone, 1989). The Tpeak reflects the maximal temperature reached during the S2.

QOP developed by Graz et al. (2010) is based on the optical identification and quantification of the organic fraction after elimination of carbonate and silicate phases by hydrochloric and hydrofluoric attacks. Components are characterized by their optical properties (colour and reflectance), their forms (amorphous or figurative) and their origins (algal, phytoclastic or fossil) (Combaz, 1964; Tyson, 1995; Di Giovanni et al., 2000; Sebag et al., 2006). Three main types of organic particles have been used in this study: red or grey amorphous particles (rAP and gAP, respectively) and lignocellulosic fragments (LCF), whose significations are given from analyses results (see below Sect. 4.3.).

4 Results

4.1 Seismic basin analysis

The bathymetric map of Lake Ledro (Fig. 2b) has been calculated interpolating the seismic data (Fig. 2a) and highlights the occurrence of steep slopes surrounding a relatively wide and flat central basin. The morphology of the glacial or bedrock substrate is seismically imaged in many areas and suggests that the sediment infill reaches a thickness of more than 40 m in the central basin (Fig. 2c). Downlapping geometries just basinward from the western and southern areas lacking seismic penetration indicate prograding beds from the Massangla and Pur river deltas, respectively (Fig. 2c). In the deepest part of the basin, sediments are thickest, well stratified and characterized by high-amplitude reflections, which have a spacing that becomes thinner towards the eastern edge of the basin (Fig. 2c). Some reflections (such as J, Fig. 2) delimited by

deltas and bedrock on the northern coast are defined by forming the top of transparent thin units whose extensions are limited by onlap configurations toward the eastern edge of the central basin (Fig. 2d).

Many transparent to chaotic lens-shaped bodies of various sizes are also present and coeval within the lacustrine basin. Events 4 and 11 (Fig. 2) are for instance described by nine and ten coeval independent bodies, which are interpreted to be the result of mass-wasting processes along the subaquatic slopes (e.g. Schnellmann et al., 2002). The thicker lens-shaped bodies (event 11) turn into a thin layer bearing few discontinuous reflections in the deepest part of the lake. The reflections connecting the tops of all coeval mass-wasting deposits are picked as seismic-stratigraphic horizons for each event, respectively (Fig. 2). They represent isochrones and coincide with sedimentary events (SE) recognized in LL082 and LL081. The event horizon can be traced throughout the lake basin, except in windows of no acoustic penetration. They also allow seismic-to-core correlations between the two coring sites (Fig. 2d).

4.2 Physical properties of sedimentary events

Cores LL081 and LL082 are composed of Holocene sedimentary sequences (for age model, see Vannière et al., this issue) of 6.9 m and 11.70 m length, respectively. Below 620 and 970 cm core depth (i.e. before 9000 cal. yr BP) in cores LL82 and LL81, respectively, the background sediment is not laminated and is only interrupted by few SE (Fig. 3a). After 9000 cal. yr BP, the succession becomes finely laminated and the occurrence of SE increases (Fig. 3a). Cumulative SE represents almost 5 and 2.5 m length of the Holocene sequence in LL082 and LL081, respectively. Two kinds of SE are easily identified from the Holocene background sediment based on their colour (dark or light), texture (graded or massive) and density data. As discussed in Vannière et al. (this issue), the identification of these two types of SE at both coring sites highlights a good core-to-core correlation between LL081 and LL082 and suggests that these SE usually affect a major part of the deep basin since only few layers are only documented in LL082, as for example the light-coloured deposit 1 (Fig. 3a). Because all these SE

are generally characterized by higher densities than the background sediment, their frequent occurrence in the basin fill can explain the relative high-amplitude reflections identified with a high-frequency on seismic data in the entire deep basin.

Dark-coloured SE are graded beds and are characterized by a sharp increase of density at their base progressively decreasing towards the top (Figs. 3b and 4a). Some organic debris were identified within these dark-coloured SE and sampled for radiocarbon dating (cf. Vannière et al, this issue). Mean grain size in most of these dark-coloured SE highlights the development of inverse (coarsening upward) and normal (fining upward) grading (from 44 to 64 and then 4 µm, and from 31 to 39 and then 2 µm, in events D and I respectively; Fig. 4a). Some dark-coloured SE are however only characterized by normal grading (e.g. from 35 to 6 µm in event G, Fig. 4a). In addition, all dark-coloured SE are not well sorted (sorting values > 2), but sorting is always increasing at the top of the deposits and associated with the formation of a thin clay cap (Fig. 4a). Dark-coloured SE thicker than 1 cm are relatively frequent (73 events during the Holocene), have a wide range of thicknesses (from 1 to 38 cm) and are on average 4.57 cm thick.

Light-coloured SE thicker than 1.5 cm are comparatively less frequent (13 events during the Holocene), less variable in thicknesses (ranging from 1.5 to 13 cm) and slightly thicker on average (5.25 cm). They are in addition much more massive both in terms of mean grain size and density (Figs. 3c and 4b). These light-coloured SE are also made of smaller particles (mean grain-size < 25 µm, Fig. 4b) than dark-coloured SE (mean grain-size < 30 µm, Fig. 4a).

4.3 Soil and lacustrine sediments organic characterisation

Soils in the drainage basin vary strongly according to elevation. High-altitude thin soils are present above 1100 m a.s.l. They are not much developed as they show no accumulation or eluviation layers, are rich in calcareous gravels and do not exceed 30 cm in thickness. They form on the calcareous bedrock and are composed of two main silty or sandy layers associated with various amounts of calcareous gravels ranging from 0 to

15 %. Well-developed soils are found between 800 and 1100 m a.s.l. They are located in forested areas, do not exceed 70 cm in thickness and form over fissured limestone which contributes to a variable gravel-content ranging from 0 to 80 % of various size (from gravels to blocks). Finally, alluvial soils are found in the alluvial plain of the flat valleys. They are characterized by a silty texture and can reach 80 cm in thickness.

The S2 (i.e. the amount of hydrocarbon that escapes from the sample during the thermal cracking) *versus* TOC (i.e. Total organic Carbon) diagram of soil and river-bed samples show that for various TOC content (ranging from 0.09 to 29.4 %) all samples are systematically near or below the line representing HI (i.e. Hydrogen Index, see Sect. 3) equals to 300 mgHC g^{-1} TOC (Fig. 5a). In agreement with Sebag et al. (2005), S2 curves from soil samples can be linked to the vegetation cover: in superficial layers from grassland soils within the drainage basin of Lake Ledro, the chart S2 *versus* temperature shows a unimodal symmetric curve with Tpeak around 462 °C, whereas in superficial layers from forested soils, the chart shows a bimodal dissymmetric curve with Tpeaks around 378 and 455 °C (Fig. 5b).

Excluding the standard, which was deliberately added into preparations, QOP (i.e. Quantitative Organic Petrography) highlights that watershed samples are composed of two major groups of organic particles: (1) non-pollen microfossil particles, consisting of colloidal red amorphous particles defined by diffuse external limits and without internal structures (rAP, Fig. 5c), cuticles and ligno-cellulosic fragments (LCF, Fig. 5c) and opaque particles without high reflectance; and (2) pollen microfossil particles composed of spores and pollens.

Holocene lacustrine samples from core LL082 (black triangles in Fig. 3a) were taken from the SE and the background sediment (i.e. in sediment layers which not correspond to SE). SE (white triangles and black squares in Fig. 6a) are always defined by HI values inferior to 300 mgHC g^{-1}TOC and thus systematically lower than background sediment samples (for the same TOC) whose HI values are higher than 300 mgHC g^{-1}TOC (white diamonds in Fig. 6a). Regression lines are calculated for background sediment and dark-coloured SE samples and show that light-coloured SE

are not identified by a specific domain but are located between the two others. The matrix effect is shown by the positive x intercept of the regression lines and is equal for background sediment and dark-coloured SE samples, representing 0.3 % of TOC. QOP performed on the same set of lacustrine samples only differs from the watershed samples by the presence of grey amorphous particles (gAP, Fig. 5c). However, the proportion of rAP, gAP and LCF is different between background-sediment and SE since background-sediment samples and light-coloured SE are mainly composed of gAP (in mean, gAP = 65 %, rAP = 13 % and LCF = 22 %), whereas dark-coloured SE are essentially composed of rAP (in mean, rAP = 59 %, gAP = 12 % and LCF = 29 %, Fig. 6b). Only two dark-coloured SE samples are dominated by gAP and correspond to samples rich in clays at the top of the deposit (clay cap; Figs. 4a and 6b, red squares).

5 Discussion

5.1 Origins of sedimentary events

As shown in Figs. 5 and 6, the organic fraction of background sediments in Lake Ledro is composed of LCF, rAP and gAP, while soils and river-bed samples are only composed of rAP and LCF. The rAP and the LCF identified in this study are similar to those described by Di Giovanni et al. (1998), Sebag et al. (2006) or Graz et al. (2010) and associated with soil particles (rAP) and upper vegetation debris (LCF) coming both from the watershed. Their occurrence in sediments from Lake Ledro is thus resulting from runoff processes in the drainage basin. The gAP are only found in lacustrine sediment samples and typically resulting from lacustrine algal productivity (Sifeddine et al., 1996; Di Giovanni et al., 1998).

This optical organic identification is also in agreement with RE results since (i) all HI values below 300 mgHC g^{-1}TOC are measured in soils and river-bed samples and characteristic of a terrestrial pole (Millet et al., 2007) and (ii) intermediate HI values of background lacustrine sediment samples are lying between the

algal pole (750 mgHC g^{-1}TOC, Talbot and Livingstone, 1989) and the terrestrial one (300 mgHC g^{-1}TOC).

5.1.1 Light-coloured SE and earthquakes

Light-coloured SE are mainly composed of algal particles similar to the ones observed throughout the background sediment suggesting a common origin. HI values (< 300 mgHC g^{-1}TOC) do not correspond here with higher terrestrial inputs but specify that the organic matter in these light-coloured SE is more degraded than in the background sediments. This oxidation suggests that light-coloured SE consist of redeposited background lacustrine sediment that became mobilized and oxidized in the water column. This interpretation is in agreement with the seismic data indicating that these light-coloured SE are restricted to the central basin but are contemporaneous to several subaquatic mass-wasting events affecting the steep slopes of the lake (Figs. 2, 7d, e). The constant mean grain-size and the stable values of sorting in these light-coloured SE (Fig. 4b) are in addition typical of mass-flow deposits (Mulder and Cochonat, 1996) so that they are therefore interpreted as distal mass-flow deposits, except for event 1 only identified in core LL082 (Fig. 3a), which is composed of tilted finely laminated sediments. This event 1 is too thin (12 cm thick) to be clearly identified on seismic data, but appears contemporaneous to hummocky morphologies identified on the eastern and northern parts of the basin (Fig. 2).

As discussed in Vannière et al (this issue), radionuclide measurements in core LL082 revealed that event 1 consists of a superposition of two equal recent sedimentary sequences. All together these characteristics of event 1 are typical from the initial stage of a thin slide deposit in the central basin favoured by a limited displacement of recent sediments along several slopes of the lake basin (i.e. creeping phenomena developing hummocky morphologies). This event 1 is dated to 2005 AD ± 3 and contemporary to the Salo earthquake in 2004 AD located at only 35 km SW from Lake Ledro (Fig. 1a, Tables 1 and 2). This earthquake could therefore be the trigger for the development

of creeping along the slopes and the formation the slide event 1 in the central basin (Fig. 8).

Two further mass-flow deposits, reaching at least 1.5 cm in thickness in the sediment cores (Fig. 8, events 2 and 3), are dated to 1870 AD ± 40 and 1860 AD ± 40 and are synchronous, within the dating error of the sediment core, with two historic earthquakes from 1901 AD and 1891 AD, respectively (Fig. 1a, Tables 1 and 2). Light-coloured SE 4 (Fig. 4b) is dated to 905 ± 130 cal. yr BP (1045 AD ± 130) and associated with numerous coeval mass movements along the basin slopes (Fig. 7d, Table 2) ~~that~~ is the typical signature of large ~~historical~~ earthquakes in lakes (Schnellmann et al., 2002; Lauterbach et al., 2012). Lake Ledro is located only 50 km NE from Verona (Fig. 1a) where a catastrophic seismic event occurred in 1117 AD (Table 1, Guidoboni and Comastri, 2005), and it is nearby the Adige valley impacted by an earthquake in 1046 AD (Fig. 1a, Table 1, Guidoboni et al., 2007). Event 4 could therefore be the consequence of one of these two regional historical earthquakes. In core LL082, pre-historical mass-flow deposits thicker than 1.5 cm are dated to 1255 ± 115, 2545 ± 105, 2595 ± 100, 3350 ± 80, 3815 ± 85, 4740 ± 155, 7190 ± 130, 9185 ± 85 and 11 495 ± 340 cal. yr BP, respectively (Table 2, Fig. 8). Some of them are, within the age-depth model errors, synchronous with pre-historical earthquakes recorded in nearby Lake Iseo (2430 ± 105, 2545 ± 105, 2595 ± 100 and 4745 ± 155 cal. yr BP, Figs. 1a and 8, Lauterbach et al., 2012) and suggest that they were triggered by large regional earthquakes (Table 2). The others light-coloured mass-flow deposits in Lake Ledro are supposed to correspond to previously undocumented local earthquakes around 3350 ± 80; 3815 ± 85; 7190 ± 130; 9185 ± 85 and 11 495 ± 340 cal. yr BP (Table 2). Event 11, dated between 5800 and 5980 cal. yr BP, has probably a seismic origin since this event is associated with the largest coeval mass-movements (Figs. 2c and 7e) that occurred in Lake Ledro during the Holocene (Table 2). Among the 14 seismic events recorded in Lake Ledro during the Holocene (Fig. 8, Table 2), ten events occurred during the last 5000 yr, i.e. during a period characterised based on a series of littoral cores by higher lake levels (Magny et al., 2012)

(Figs. 2b and 8). These higher levels may have therefore favoured slope instabilities and increased the sensitivity of Lake Ledro to regional seismo-tectonic activity.

5.1.2 Dark-coloured SE and flood deposits

Dark-coloured SE in Lake Ledro present the same organic signature as that of the watershed samples since they are essentially composed of terrestrial components similar to the ones identified throughout the drainage basin (rAP and LCF, Fig. 5b) and characterized by HI values clearly below 300 mgHC g^{-1}TOC. In addition, laser grain-size and bulk-density measurements in these beds clearly indicate that most of their bases are successively inversely and normally graded. This is the typical signature of hyperpycnal flood deposits in a subaquatic basin (Mulder and Alexander, 2001; Mulder et al., 2003; Mulder and Chapron, 2011; Saint-Onge et al., 2012), where the coarsening-upward and the fining-upward sequences are correlated to the rising and the falling limb of a flood hydrograph, respectively. The very thin basal unit of event J, compared to the thick upper unit, implies therefore an asymmetric flood hydrograph which is typical of hyperpycnites and corresponds to the succession of the waxing and waning flows (Saint-Onge et al., 2004; Mulder and Chapron, 2011). Because the preservation of the waxing unit of a hyperpycnite at a given location in a basin is typically linked to (i) the flood hydrograph, (ii) the peak intensity of the flood event and (iii) the proximity of the tributary (Mulder et al., 2003), dark-coloured SE characterized only by a fining upward sequence (such as event G) at coring sites LL081 and/or LL082 in Lake Ledro can be related to exceptional flood events whose peak intensities were high enough to erode the waxing unit. In addition, the significant occurrence of algal particles in the clay caps of dark-coloured SE is interpreted as resulting from the remobilization in the water column of lacustrine sediments at the lake floor during the development of the hyperpycnal current (Chapron et al., 2007). These clay caps would therefore essentially result from the settling of fine-grained particles suspended near the lake floor at the end of the flood event.

Dark-coloured SE in Lake Ledro are thus interpreted as hyperycnal flood deposits largely composed of soil material and vegetation debris eroded from the drainage basin and brought in the lake by heavy precipitation and/or snowmelt events. Because Massangla and Pur rivers are temporary torrential tributaries draining steep slopes, dark-coloured SE in Lake Ledro are likely reflecting flash-flood events (Lambert and Giovanoli, 1988; Bornhold et al., 1994; Gilli et al., 2012). The large flood deposits marked by dark-coloured SE J is thick enough to be mapped along seismic profiles (Fig. 7c). It reaches up to 6.4×10^5 m^2 of area, is extending from the Massangla and Pur delta slopes towards the central basin where it forms an up to 50 cm thick depocenter (Fig. 7b) and develops onlaping geometries at the eastern edge of the central basin (Fig. 7c).

5.2 Flood events and soil erosion

Since flood deposits in Lake Ledro are essentially composed of soil-derived material, it is necessary to estimate the amount of pedological material eroded during exceptional flood events from the catchment area, in order to test if their occurrence in the lake basin can be used as a good proxy to reconstruct the paleohydrology of the study area.

The spatial extensions of the hyperpycnal floods recorded into Lake Ledro are given by their eastern onlap configurations of their high-amplitude reflections in the central basin (Figs. 2d and 7c). Densities of soil surface-layers sampled in the catchment area vary from 1.04 to 1.7 g cm^{-3} (on average 1.3 g cm^{-3}) and are close to ones measured in flood deposits from sediment cores (on average 1.4 g cm^{-3}). The calculated volume of terrestrial fine fraction eroded during a flash-flood is thus assumed as representative of the total terrestrial material eroded within the erodible surface of the catchment area. It is calculated multiplying the mean thickness of a specific dark-event deposit by the mean spatial extent of Lake Ledro hyperpycnal flood events (evaluated to 3.3×10^5 m^2 on average, Fig. 7b) and by the percentage of terrestrial material inside (determined by QOP). This volume represents mechanical erosion of an unknown thickness of soil

within a certain percentage of the erodible surface source of terrestrial material. De Ploey (1991), Cerdà (1998, 1999), Le Bissonnais et al. (2001), Souchère et al. (2003) and Girard et al. (2011) described that the cumulative effects of gullying on the thalwegs and on slopes steeper than 30 % are the two main factors controlling soil erosion within a drainage basin under a given vegetation cover. Analysing the digital elevation model, we consider that the topography was constant during all the Holocene period and intersect the two key criterions (thalwegs and slopes > 30 %, Fig. 1b, orange and yellow areas, respectively) in order to map source areas of terrestrial material ($\sim 23.3\,km^2$ in the catchment). Flat alluvial valleys slopes (0–5 %; Fig. 1b, hatched red areas, $0.8\,km^2$ in the catchment) are mainly sites of accumulation processes; however, the material stocked in these valleys can be remobilized during flood events (Girard et al., 2011). We consider therefore that slopes between 0 and 5 % can also be affected by erosion processes during a flash-flood event. The equivalent thickness of soil eroded corresponding to 100 % of these source areas affected by erosion represents the minimum equivalent soil thickness which can be eroded by a given flood event. It is more difficult to determine this value for thinner flood events which represent low terrestrial volumes (black curve, flood event of 2 cm thick in LL082, Fig. 9a) than for thicker events (grey curve, flood event J, 38 cm thick in LL082, Fig. 9a). The pre-historical major hyperpycnal flood event F (18 cm thick into core LL082, Fig. 10b) is the example presented in Fig. 9. It is on average composed of 0.9 % of pedological components (rAP) which correspond to $53\,460\,m^3$ of accumulated terrestrial material. Considering this volume, 2.2 mm of equivalent soil thickness, within the catchment area of Lake Ledro, are at least eroded by this flash-flood event (blue curve, Fig. 9a). Similarly we can estimate that events G and J (Fig. 10b) eroded at least 2.6 mm and 4 mm of equivalent soil thickness in the watershed of Lake Ledro, respectively.

This approach highlights that extreme events eroded at least few millimetres of soil over the watershed and correspond to values described by Raclot and Albergel (2006) for areas affected by modern water erosion and runoff. Their recurrence in time can be problematic and can affect the pedogenesis process at long time scales since

Duchaufour (1983) stated that well-developed soil pedogenesis as those described in Lake Ledro catchment area is relatively slow. However, events F, G and J are exceptional in intensity since they are the only ones to reach such thicknesses during the Holocene. This indicates that the pedogenesis in Lake Ledro watershed is not significantly affected by the recurrence of flash-flood events and suggests that Lake Ledro flood sequence offers a reliable record to track the evolution of precipitation regimes during the Holocene in this part of the Alps.

5.3 Climatic significance of flash-flood deposits in Lake Ledro

It is well known that rainfall events have to reach a certain threshold in magnitude, duration, intensity or discharge to trigger erosional processes and flooding in drainage basins (De Ploey et al., 1995; Mudelsee et al., 2003; Marchi et al., 2010). According to Mulder et al. (2003) there is also a positive relationship between the flood-deposit thickness, the river discharge and the rain intensity. The De Ploey erosional susceptibility approach is an elementary model which considers that the volume of soil eroded during a storm event is directly proportional to the amount of precipitation received under a given vegetation cover and function of the slope, the parent material and the actual annual mean of precipitation (De Ploey, 1991, 1995). A direct application of De Ploey model to pre-historical major hyperpycnal flood events F, G and J in Lake Ledro, suggests that the maximal amount of precipitation needed to erode the minima equivalent soil thicknesses by each flood event are equal to 1710 mm, 1650 mm and 2045 mm, respectively (Fig. 9b).

This estimated precipitation of single storm events is two times the volume received today in one year in the Trento region and suggests that rainfall cannot be the only source of water to generate such phenomena. De Ploey calculations are in fact only corresponding to a cumulative volume of fluid needed to induce soil erosion and runoff. Because several recent studies focusing on modelling of snowmelt erosion have shown that this process could export a large amount of soil particles (60 %) especially on grasslands where the snowmelt runoff coefficient is higher (Ollesch et al., 2006;

Tanasienko et al., 2009, 2011), we suggest that Holocene flash-flood deposits in Lake Ledro are resulting from the combination of heavy rainfalls and snowmelt phenomena. This interpretation is further supported by the stratigraphic position of flash-flood deposits within the finely laminated background sediments of Lake Ledro (Fig. 3a): on digital photographs flash-flood deposits are systematically caped by a white lamina during the first half of the Holocene and by a brownish lamina after around 5000–4500 cal. yr BP (Fig. 3a). Following Wirth et al. (2012) who demonstrated that Lake Ledro basin fill was composed of biogeochemical varves (cf. Lotter et al., 1997) over the last 1400 yr, and assuming that varves formation prevailed since the onset of finely laminated background sediments ca. 9000 cal. yr BP, we can hypothesize that flash-flood events in Lake Ledro occurred in spring during the first half of the Holocene (i.e. before the white summer layer made of authigenic calcite) and between late fall and winter, after around 5000–4500 cal. yr BP (i.e. before the brownish winter layer made of organic and clay particles). The analysis of further thin sections (cf. Mangili et al., 2005) are however required to confirm the precise seasonality of flash-flood events in Lake Ledro during the Holocene.

5.3.1 Climate and human interactions on terrestrial and lacustrine Holocene environment at Lake Ledro

The most important parameters discussed below are depicted in Fig. 10. In a first time, the hyperpycnal flood occurrences and thicknesses documented by Lauterbach et al. (2012) in nearby Lake Iseo (Figs. 1a and 10a) are compared to the hyperpycnal flood occurrences and thicknesses identified in Lake Ledro (Fig. 10b). This comparison suggests the occurrence of wetter periods favouring flooding activity at a regional scale in the Italian Southern Alps (Fig. 10). During the first half of the Holocene, the mean flood intervals from lakes Iseo and Ledro are equalled to 4.8 and 4 events by millennia, respectively, whereas after around 5000 cal. yr BP, they increased to 8.4 and 9.2 events by millenia, respectively. These changes in flood return times suggest that (i) the two lakes are sensitive to the same climatic influences and that (ii) the

second half of the Holocene was wetter, which is in agreement with the higher lake-levels documented by Magny et al. (2009, 2012) at Lake Ledro. Over the last 500 years, the last wetter period recorded by hyperpycnal flood deposits in the Southern Alps (Fig. 10b) occurred between ca. 1600 AD and 1850 AD and matches the second phase of the well-documented Little Ice Age period (Chapron et al., 2002; Wanner et al., 2011; Magny et al., 2010).

In a second time, variations in the values of the rAP/LCF ratio obtained by QOP (i.e. Quantitative Organic Petrography) for background sediments (white circles, Fig. 10c) and for flood SE (black circles, Fig. 10c) are represented. This ratio can be used to disentangle the impact of land-use and climate during the Holocene on the vegetal cover, soil erosion and sediment load of rivers in Alpine environments (cf. Noël et al., 2001; Arnaud et al., 2005; Dearing, 2006; Dearing et al., 2006; Jacob et al., 2009). Indeed, this ratio, measured in the background sediment, can be used to track the long-term evolution of the vegetation cover within a watershed, using the respective contribution of soil (rAP) and litter (LCF) material in the terrestrial organic matter fluxes delivered to the lake by runoff on topsoil layers (Di Giovanni et al., 2000). Values of the ratio rAP/LCF, measured in flood SE, can reflect either the source areas of material eroded during a flood event or its seasonality if the vegetal cover in the watershed is depending on the seasons. The significance of the rAP/LCF ratio in flood SE is further supported by the shape of the S2 curves from flood SE samples which can be typical of grassland or forest soils (i.e. Sect. 4.3., unimodal or bimodal S2 curves, respectively in Fig. 10d). Finally, algal and terrestrial contributions in the background sediment (white circles, Fig. 10e) and in the flood SE (black circles, Fig. 10e) are estimated from the HI values trends (i.e. Hydrogen Index, see Sect. 3).

5.3.2 During the Early Holocene: from 10 000 to 8000 cal. yr BP

Between 10 000 and 8000 cal. yr BP, the ratio rAP/LCF from background sediment fluctuated (white circles, Fig. 10c) resulting from variations in litter and soil particles supply. HI values (Fig. 10e) show exactly the same trend. This pattern suggests that

the soils present through the drainage basin of Lake Ledro was not stabilized yet and that runoff processes could affect grassland areas (essentially delivering rAP particles) as well as forested ones (essentially delivering LCF particles). This is in agreement with Magny et al. (2012) and Joannin et al. (this issue) who documented the progressive reforestation of the area during this period. Around 8200–8000 cal. yr BP, high values of the rAP/LCF ratio are measured in background sediment samples. This indicates a period of enhanced grassland soil erosion which matches a cold and wet period such as the 8.2 event, frequently documented in western Europe (von Granfenstein et al., 1999) and notably at Lake Ledro (Magny et al., 2012).

In flood events, the ratio rAP/LCF is always high (black circles, Fig. 10c) suggesting that soil particles (rAP) are essentially exported. S2 curves from the flood events dated from this period are unimodal and symetric (Fig. 10d) and therefore typical of runoff on superficial layers from grassland soil suggesting that high altitude areas (or still not reforested ones) were preferentially affected by flash-floods during the Early Holocene.

5.3.3 During the Mid-Holocene: from 8000 to 4200 cal. yr BP

Between 8000 and 4200 cal. yr BP, the ratio rAP/LCF from background sediment is low (white circles in Fig. 10c) indicating that litter material is preferentially exported comparing to soil particles by runoff processes. This suggests (i) that the catchment area of Lake Ledro was essentially forested during this period, which is in agreement with Joannin et al. (this issue) and (ii) that this reforestation stabilized the soils. The lower erosion rate documented here is further supported by the lower lake-levels documented by Magny et al. (2009, 2012) at Lake Ledro during this period. Indeed, these conditions resulted from a drier and warmer climate which among others limited the runoff. HI values (Fig. 10e) are higher than 300 mgHC g^{-1}TOC over this period, reflecting both the lower soil supply into lake sediment and the higher contribution of lacustrine algal production (correlation between HI and algal productivity: $R = 0.67$, $p < 0.001$), certainly favoured by the warmer climate.

In flood SE, the ratio rAP/LCF is high (black circles, Fig. 10c) and the shape of the S2 curve is unimodal and symmetric (Fig. 10d) during this second period. This indicates that during the Mid-Holocene, the organic material exported during flood events is still essentially made of soil particles from grassland (high-elevated) areas.

5.3.4 During the Late Holocene: from 4200 to 3100 cal. yr BP

Between 4200 and 3100 cal. yr BP, the high rAP/LCF ratio in Lake Ledro background sediment reflects enhanced soil erosion from non-forested areas topsoils. This is further supported by the HI values measured in background sediment which decrease below 300 mgHC g^{-1}TOC (Fig. 10e) suggesting higher terrestrial contribution into lake sediment by runoff processes (correlation between HI and soil particles: $R = 0.71$, $p = 0.03$). Moreover, this higher terrestrial supply is contemporaneous to the increase of lacustrine sediment magnetic susceptibility interpreted by Vannière et al. (this issue) as the result of higher soil erosion. These results probably reflect the cumulative effects of (i) the climate shift to wetter conditions (Magny et al., 2012) and thereby higher runoff and of (ii) the human-induced land openness documented by Joannin et al. (this issue). Indeed, this time interval is matching a period of well-documented human settlements along the shores of several lakes from the Southern Alps, including Lake Ledro (Magny et al., 2009, 2012, Fig. 2b). Bronze Age in Italy is in particular known for a sustained increase in human impact (Cremashi et al., 2006). These human-induced soil destabilisations could favour the soil erosion under wetter climatic conditions.

In flood SE, a high rAP/LCF ratio is measured (Fig. 10c) suggesting that the material from open landscapes ~~were~~ remobilized. However, the shape of the S2 curve from flood deposits is bimodal and dissymmetric (Fig. 10d) and therefore typical of forested areas. These two results suggest that the superficial layers from former forested soils were preferentially destabilized and eroded during the Bronze Age flash-flood events. Both the increase of the mean flood interval from 4 to 9.2 events by millennia (Fig. 10b) and

the increasing thickness of the floods recorded in the central basin of Lake Ledro during this period (events F and G for example, Fig. 10b) may thereby have resulted from a combination of more humid climate conditions and human-induced soil destabilization and erosion.

5.3.5 During the Late Holocene: from 3100 to present-day

During the time interval 3100–1200 cal. yr BP, the ratio rAP/LCF from background sediment and flood deposits is progressively dropping (Fig. 10c), suggesting reduced soil particles erosion over the catchment area which is in agreement with the slight drop in zirconium influx coming from soil erosion documented by Vannière et al. (this issue). This reduction of erosion processes could indicate a certain stabilization of the soil within the drainage basin or changes in human land-use. After 1200 cal. yr BP, the interpretation of the ratio rAP/LCF in background sediment is however becoming more difficult. The lower values of the ratio rAP/LCF seem to indicate that the erosion processes essentially exported litter material from forested topsoil layers (Fig. 10c). During the same time-interval, Vannière et al. (this issue) described higher minerogenic supply coming from soil erosion (zirconium influx) and land openness from 950 cal. yr BP. Both increase in minerogenic supply and decrease in rAP/LCF ratio in background sediment are typical of the remobilization of deeper soil layers where the rAP/LCF ratio is constant whatever the vegetation cover (Graz et al., 2010). In this case, both minerogenic and organic results suggest drastic landscape disturbances over the catchment probably associated with ploughing activities and intensive human impact that affected deeper soil layers over the last millennium.

In flood SE, a low rAP/LCF ratio is also measured (Fig. 10c) and the shape of the S2 curve from flood deposits is bimodal and dissymmetric (Fig. 10d) which is typical of forested areas. Combined with our previous hypothesis on the background sediment signal, these two results suggest that the deeper layers from former forested soils could

be destabilized and eroded during recent flood SE. Moreover, frequent but finer hyperpycnal flood deposits are recorded during this period (Fig. 10b). They may result from an anthropogenic reorganisation of the drainage basin. The last hyperpycnal flood deposit recorded in our sediment cores is dated to 1920 AD ± 20 and is 2 cm thick. It is interesting to note that Lake Ledro does not record any other hyperpycnal flood after this date. This suggests either a primary climate signature (Pfister, 2009), or that regulating activities during hydropower production since 1929 AD can modify the temperature of the water column and maybe prevent from generation of hyperpycnal flood or more probably that recent human infrastructure on river corrections in the catchment area have been very efficient to reduce the impact of flash-flood events on lacustrine environments.

6 Conclusions

In Lake Ledro, the combination of high-resolution seismic profiling with physical and organic analyses of sediment cores, soils and river-bed samples allows (i) characterizing the sensitivity of Holocene lacustrine sedimentation to changes in vegetation cover within the drainage basin and (ii) distinguishing the origins of the contrasted sedimentary events which regularly interrupted the background sedimentation. Up to 73 catastrophic hyperpycnal flood deposits (> 1 cm) resulting from the combination of heavy rainfalls with snowmelt have especially been discriminated from 14 subaquatic mass-wasting deposits.

Distal mass-flow deposits in the central basin of Lake Ledro are generally associated with numerous coeval mass-movements along the steep slopes of the basin affecting not only deltaic environments. The chronology of these coeval mass movements matching either historical regional earthquakes (in 2004; 1901; 1891 and 1117 or 1046 AD) or coeval mass-movements in nearby Lake Iseo documented by Lauterbach et al. (2012) around 2525 ± 110 and 4490 ± 110 cal. yr BP, is providing new

evidences that the Southern Italian Alps have been frequently affected by large regional earthquakes. Similar coeval mass-movements dated around 3350 ± 80; 3815 ± 85; 5890 ± 90; 7190 ± 130; 9185 ± 85 and 11 495 ± 340 cal. yr BP are supposed to be related to previously undocumented (and eventually more local) earthquakes.

The longterm evolution of the vegetation cover in the drainage basin of Lake Ledro has been deduced from the respective contributions of soil and litter fluxes delivered to the lake by runoff in background sediments. During the first half of the Holocene, the drainage basin was forested and hyperpycnal floods occurring during springs essentially affected grassland areas. Inversely, after around 5000–4500 cal. yr BP, climate variability favoured the development of flash-floods during the snow season and the intensification of human activities increased soil erosion, especially between 4000 and 3100 cal. yr BP. Enhanced occurrence of natural hazards such as earthquakes and flash-floods during this period may have, in addition, contributed to the decline of the lake-dwelling at Lake Ledro. Our results also suggest that over the last millennium, changes in human land-use, such as ploughing activities, may have affected the deeper soil layers.

This study highlights that if present-day climate or modern river corrections apparently succeeded to diminish the development of hyperpycnal flood events in Lake Ledro: land use combined with future climate changes may have irreversible consequences on soil erosion and on the pedogenesis preserved until now.

Acknowledgements. We would like to warmly thank Marielle Hatton and Rachel Boscardin from ISTO for their support during the analyses of organic matter samples, Laurent Perdereau from ISTO for his contribution to the processing of seismic data and Romana Scandolari and Luca Scoz from the Molina di Ledro museum for logistical support during field work operations and fruitful scientific discussions. Seismic data interpretation and mapping has been performed using the Kingdom Software® from Seismic Micro-Technology Inc. (SMT). Financial support for this study was provided by the French ANR (project LAMA, M. Magny and N. Combourieu-Nebout) and the Swiss National Science Foundation (project FloodAlp; Grant 200021-121909).

The publication of this article is financed by CNRS-INSU.

References

Ariztegui, D., Chondrogianni, C., Lami, A., Guilizzoni, P., and Lafargue, E.: Lacustrine organic matter and the Holocene paleoenvironmental record of Lake Albano (central Italy), J. Paleolimnol., 26, 283–292, 2001.

Arnaud, F., Revel, M., Chapron, E., Desmet, M., and Tribovillard, N.: 7200 years of Rhone river flooding activity in Lake Le Bourget, France: a high-resolution sediment record of NW Alps hydrology, The Holocene, 15, 420–428, 2005.

Barredo, J. I.: Major flood disaster in Europe: 1950–2005, Nat. Hazards, 42, 125–148, 2007.

Behar, F., Beaumont, V., and De B. Penteado, H. L.: Rock-Eval 6 Technology: performances and Developments, Oil Gas Sci. Technol., 56, 2, 111–134, 2001.

Beniston, M., Stephenson, D. B., Christensen, O. B., Ferro, C. A. T., Frei, C., Goyette, S., Halsnaes, K., Holt, T., Jylhä, K., Koffi, B., Palutikol, J., Schöll, R., Semmler, T., and Woth, K.: Future extreme events in European climate: an exploration of regional climate model projections, Climatic Change, 81, 71–95, 2007.

Beug, H. J.: Untersuchungen zur spätglazialen Vegetationsgeschichte im Gardaseegebiet unter besonderer Berücksichtigung der mediterranen Arten, Flora, 154, 401–440, 1964.

Bøe, A. G., Dahl, S. O., Lie, Ø., and Nesje, A.: Holocene river floods in the upper Glomma catchment, southern Norway: a high-resolution multiproxy record from lacustrine sediments, The Holocene, 16, 445–455, 2006.

Bollettinari, G., Picotti, V., Cantelli, L., Castellarin, A., Trombetta, G., and Claps, M.: Carta geologica d'Italia - Riva del Garda, Foglio 080 della carta 1:50.000 dell'I.G.M., 2005.

Bornhold, B. D., Ren, P., and Prior, D. B.: High-frequency turbidity currents in British Columbia fjords, Geo-Mar. Lett., 14, 238–243, 1994.
Buma, J. and Dehn, M.: A method for predicting the impact of climate change on slope stability, Environ. Geol., 35, 190–196, 1998.
Calvert, S. E.: Beware intercepts: interpreting compositional ratios in multi-component sediments and sedimentary rocks, Org. Geochem., 35, 981–987, 2004.
Cerdà, A.: The influence of geomorphological position and vegetation cover on the erosional and hydrological processes on a Mediterranean hillslope, Hydrol. Process., 12, 661–671, 1998.
Cerdà, A.: Parent Material and Vegetation Affect Soil Erosion in Eastern Spain, Soil Sci. Soc. Am. J., 63, 362–368, 1999.
Chapron, E., Beck, C., Pourchet, M., and Deconninck, J. F.: 1822 earthquake-triggered homogenite in Lake Le Bourget (NW Alps), Terra Nova, 11, 86–92, 1999.
Chapron, E., Desmet, M., De Putter, T., Loutre, M. F., Beck, C., and Deconinck, J. F.: Climatic variability in the northwestern Alps, France, as evidence by 600 years of terrigenous sedimentation in Lake Le Bourget, The Holocene, 12, 177–185, 2002.
Chapron, E., Arnaud, F., Noël, H., Revel, M., Desmet, M., and Perdereau, L.: Rhone River flood deposits in Lake Le Bourget: a proxy for Holocene environmental changes in the NW Alps, France, Boreas, 34, 404–416, 2005.
Chapron, E., Juvigné, E., Mulsow, S., Ariztegui, D., Magand, O., Bertrand, S., Pino, M., and Chapron, O.: Recent clastic sedimentation processes in Lake Puyehue (Chilean Lake District, 40.5° S), Sediment. Geol., 201, 365–385, 2007.
Christensen, J. H. and Christensen, O. B.: Climate modelling: Severe summertime flooding in Europe, Nature, 421, 805–806, 2003.
Combaz, A.: Les palynofaciès, Revue de Micropaléontologie, 7, 205–218, 1964.
Copard, Y., Di Giovanni, C., Martaud, T., Albéric, P., and Olivier, J. E.: Using Rock-Eval 6 pyrolysis for tracking fossil organic carbon in modern environments: implications for the roles of erosion and weathering, Earth Surf. Proc. Land., 31, 135–153, 2006.
Cremaschi, M., Pizzi, C., and Valsecchi, V.: Water management and land use in the terramare and a possible climatic co-factor in their abandonment: The case study of the terramara of Poviglio Santa Rosa (northern Italy), Quaternary Int., 151, 87–98, 2006.
Dearing, J. A.: Climate-human-environment interactions: resolving our past, Clim. Past, 2, 187–203, doi:10.5194/cp-2-187-2006, 2006.

Dearing, J. A., Battarbee, R. W., Dikau, R., Larocque, I., and Oldfield, F.: Human-environment interactions: learning from the past, Reg. Environ. Change, 6, 1–16, 2006.
Debret, M., Chapron, E., Desmet, M., Rolland-Revel, M., Magand, O., Trentesaux, A., Bout-Roumazeille, V., Nomade, J., and Arnaud, F.: North western Alps Holocene paleohydrology recorded by flooding activity in Lake Le Bourget, France, Quaternary Sci. Rev., 29, 2185–2200, 2010.
De Ploey, J.: Bassins versants ravinés: analyses et prévisions selon le modèle Es, Bulletin de la Société géographique de Liège, 27, 69–76, 1991.
De Ploey, J., Moeyersons, J., and Goosens, D.: The De Ploey erosional susceptibility model for catchments, Es, Catena, 25, 269–314, 1995.
Di Giovanni, C., Disnar, J. R., Campy, M., Bichet, V., and Guillet, B.: Geochemical characterization of soil organic matter and variability of a post glacial detrital organic supply (Chaillexon lake, France), Earth Surf. Proc. Land., 23, 1057–1069, 1998.
Di Giovanni, C., Disnar, J.R., Bichet, V., and Campy, M.: Seasonal variability and threshold effects of the organic detrital sedimentation in lakes: imbalances between organic records and climatic fluctuations (Chaillexon basin, Doubs, France), B. Soc. Geol. Fr., 171, 533–544, 2000.
Disnar, J. R., Guillet, B., Keravis, D., Di Giovanni, C., and Sebag, D.: Soil organic matter (SOM) characterization by Rock-Eval pyrolysis: scope and limitations, Orga. Geochem., 34, 327–343, 2003.
Duchaufour, P.: Pédogenèse et classification 2nd Edn., Masson, Paris, 491 pp., 1983.
Espitalié, J., Deroo, G., and Marquis, F.: La pyrolyse Rock-Eval et ses applications. Première partie, Oil Gas Sci. Technol., 40, 563–579, 1985.
Fanetti, D., Anselmetti, F. S., Chapron, E., Sturm, M., and Vezzoli, L.: Megaturbidite deposits in the Holocene basin fill of Lake Como (Southern Alps, Italy), Palaeogeogr. Palaeocl., 259, 323–340, 2008.
Gilli, A., Anselmetti, F. S., Glur, L., and Wirth, S. B.: Lake sediments as archives of reccurrence rates and intensities of past flood events, in: Dating torrential processes on fans and cones - methods and their application for hazard and risk assessment, edited by: Michelle Schneuwly-Bollschweiler, M. S., Stoffel, M., and Rudolf-Miklau, F., Advances in Global Change Research, 47, Springer, 2012.
Girard, M. C., Walter, C., Rémy, J. C., Berthelin, J., and Morel, J. L.: Sols et environnements 2nd Edn., Dunod, Paris, 881 pp., 2011.

Graz, Y., Di Giovanni, C., Copard, Y., Laggoun-Défarge, F., Boussafir, M., Lallier-Vergès, E., Baillif, P., Perdereau, L., and Simonneau, A.: Quantitative palynofacies analysis as a new tool to study transfers of fossil organic matter in recent terrestrial environments, Int. J. Coal Geol., 84, 49-62, 2010.

Guidoboni , E. and Comastri, A.: The "exceptional" earthquake of 3 January 1117 in the Verona area (northern Italy): A critical time review and detection of two lost earthquakes (lower Germany and Tuscany), J. Geophys. Res., 110, 1–20, 2005.

Guidoboni, E., Ferrari, G., Mariotti, D., Comastri, A., Tarabusi, G., and Valensise, G.: Catalogue of strong earthquakes in Italy 461B.C.–1997 and Mediterranean area 760 B.C.-1500, available at: http://storing.ingv.it/cfti4med/ (last access: 15 January 2011), 2007.

Jacob, J., Disnar, J. R., Boussafir, M., Sifeddine, A., Turcq, B., and Spadano Albuquerque, A. L.: Major environmental changes recorded by lacustrine sedimentary organic matter since the last glacial maximum near the equator (Lagoa do Caçó, NE Brazil), Palaeogeogr. Palaeocl., 205, 183–197, 2004.

Jacob, J., Disnar, J. R., Arnaud, F., Gauthier, E., Billaud, Y., Chapron, E., and Bardoux, G.: Impacts of new agricultural practices on soil erosion during the Bronze Age in the French Prealps, The Holocene, 19, 241–249, 2009.

Joannin, S., Vannière, B., Galop, D., Magny, M., Gilli, A., Chapron, E., Wirth, S., Anselmetti, F. S., and Desmet, M.: Holocene vegetation and climate changes in the Central Mediterranean at Lake Ledro (Trentino, Italy), Clim. Past, submitted, 2012.

Knox, J. C.: Sensitivity of modern and Holocene floods to climate change, Quaternary Sci. Rev., 19, 439–457, 2000.

Lambert, A. and Giovanoli, F.: Records of riverborne turbidity currents and indications of slope failures in the Rhone delta of Lake Geneva, Limnol. Oceanogr., 33, 458–168, 1988.

Lauterbach, S., Chapron, E., Brauer, A., Hüls, M., Gilli, A., Arnaud, F., Piccin, A., Nomade, J., Desmet, M., and von Grafenstein, U.: A sedimentary record of Holocene surface runoff events and earthquake activity from Lake Iseo (Southern Alps, Italy), The Holocene, 22, 749–760, 2012.

Le Bissonnais, Y., Montier, C., Jamagne, M., Daroussin, J., and King, D.: Mapping erosion risk for cultivated soil in France, Catena, 46, 207–220, 2001.

Lotter, A. F., Sturm, M., Teranes, J. L., and Wehrli, B.: Varve formation since 1885 and high-resolution varve analyses in hypertrophic Baldeggersee (Switzerland), Aquat. Sci., 59, 304–325, 1997.

Magny, M.: Holocene climate variability as reflected by mid-European lake-level fluctuations and its probable impact on prehistoric human settlements, Quaternary Int., 113, 65–79, 2004.

Magny, M., Galop, D., Bellintani, P., Desmet, M., Didier, J., Haas, J. N., Martinelli, N., Pedrotti, A., Scandolari, R., Stock, A., and Vannière, B.: Late-Holocene climatic variability south of the Alps as recorded by lake-level fluctuations at Lake Ledro, Trentino, Italy, The Holocene, 19, 575–589, 2009.

Magny, M., Arnaud, F., Holzhauser, H., Chapron, E., Debret, M., Desmet, M., Leroux, A., Millet, L., Revel, M., and Vannière, B.: Solar and proxy-sensitivity imprints on paleohydrological records for the last millennium in west-central Europe, Quaternary Res., 73, 173–179, 2010.

Magny, M., Joannin, S., Galop, D., Vannière, B., Haas, J. N., Basseti, M., Bellintani, P., Scandolari, R., and Desmet, M.: Holocene paleohydrological changes in the northern Mediterranean borderlands as reflected by the lake-level record of Lake Ledro, north-eastern Italy, Quaternary Res., 77, 382–396, doi:10.1016/j.yqres.2012.01.005, 2012.

Mangili, C., Brauer, A., Moscariello, A., and Naumann, R.: Microfacies of detrital event layers deposited in Quaternary varved lake sediments of the Piànico-Sèllere Basin (northern Italy), Sedimentology, 52, 927–943, 2005.

Marchi, L., Borga, M., Preciso, E., and Gaume, E.: Characterization of selected extreme flash floods in Europe and implications for flood risk management, J. Hydrol., 394, 118–133, 2010.

Millet, L., Vannière, B., Verneaux, V., Magny, M., Disnar, J.R., Laggoun-Défarge, F., Walter-Simonnet, A.V., Bossuet, G., Ortu, E., and de Beaulieu, J. L.: Response of littoral chironomid communities and organic matter to late glacial lake-level, vegetation and climate changes at Lago dell'Accesa (Tuscany, Italy), J. Paleolimnol., 38, 525–539, 2007.

Mudelsee, M., Börngen, M., Tetzlaff, G., and Grünewald, U.: No upward trends in the occurrence of extreme floods in central Europe, Nature, 425, 166–169, 2003.

Mulder, T. and Alexander, J.: The physical character of subaqueous sedimentary density flows and their deposits, Sedimentology, 48, 269–299, 2001.

Mulder, T. and Chapron, E.: Flood deposits in continental and marine environments: character and significance, in: Sediment transfer from shelf to deep water – Revisiting the delivery system, AAPG Studies in Geology, 61, edited by: Slatt, R. M. and Zavala, C., 1–30, 2011.

Mulder, T. and Cochonat, P.: Classification of offshore mass movements, J. Sediment. Res., 66, 43–57, 1996.

Mulder, T., Syvitski, J. P. M., Migeon, S. Faugères, J. C., and Savoye, B.: Marine hyperpycnal flows: initiation, behavior and related deposits. A review, Mar. Petrol. Geol., 20, 861–882, 2003.
Muldersee, M., Börngen, M., Tetzlaff, G., and Grünewald, U.: No upward trends in the occurrence of extreme floods in central Europe, Nature, 425, 166–169, 2003.
Noël, H., Garbolino, E., Brauer, A., Lallier-Vergès, E., de Beaulieu, J. L., and Disnar, J. R.: Human impact and soil erosion during the last 5000 yrs as recored in lacustrine sedimentary organic matte rat Lac d'Annecy, the French Alps, J. Paleolimnol., 25, 229–244, 2001.
Ollesch, G., Kistner, I., Meissner, R., and Lindenschmidt, K. E.: Modelling of snowmelt erosion and sediment yield in a small low-mountain catchment in Germany, Catena, 68, 131–176, 2006.
Pfister, C.: Die "Katastrophenlücke" des 20. Jahrhunderts und der Verlust traditionalen Risikobewusstseins, GAIA, 18, 239–246, 2009.
Raclot, D. and Albergel, J.: Runoff and water erosion modelling using WEPP on a Mediterranean cultivated catchment, Physics and Chemistry of the Earth, 31, 1038–1047, 2006.
Ramanampisoa, L. and Disnar, J. R.: Primary control of paleoproduction on organic matter preservation and accumulation in the Kimmeridge rocks of Yorkshire (UK), Org. Geochem., 21, 1153–1167, 1994.
Saint-Onge, G., Mulder, T., Piper, D. J. W., Hillaire-Marcel, C., and Stoner, J. S.: Earthquake and flood-induced turbidites in the Saguenay Fjord (Québec): a Holocene paleoseismicity record, Quaternary Sci. Rev., 23, 283–294, 2004.
Saint-Onge, G., Chapron, E., Mulsow, S., Salas, M., Viel, M., Debret, M., Foucher, A., Mulder, T., Winiarski, T., Desmet, M., Costa, P. J. M., Ghaleb, B., Jaouen, A., and Locat, J.: Comparison of earthquake-triggered turbidites from the Saguenay (Eastern Canada) and Reloncavi (Chilean margin) Fjords: Implications for paleoseismicity and sedimentology, Sediment. Geol., 243–244, 89–107, 2012.
Sebag, D., Disnar, J. R., Guillet, B., Di Giovanni, C., Verrecchia, E. P., and Durand, A.: Monitoring organic matter dynamics in soil profiles by 'Rock-Eval pyrolysis': bulk characterization and quatification of degradation, Eur. J. Soil Sci., 57, 344–355, 2005.
Sebag, D., Copard, Y., Di Giovanni, C., Durand, A., Laignel, B., Ogier, S., and Lallier-Verges, E.: Palynofacies as useful tool to study origins and transfers of particulate organic matter in recent terrestrial environments: Synopsis and prospects, Earth-Sci. Rev., 79, 241–259, 2006.

Sifeddine, A., Bertrand, P., Lallier-Vergès, E., and Patience, A. J.: Lacustrine organic fluxes and palaeoclimatic variations during the last 15 ka: Lac du Bouchet (Massif Central, France), Quaternary Sci. Rev., 15, 203–211, 1996.
Schnellmann, M., Anselmetti, F. S., Giardini, D., McKenzie, J. A., and Ward, S. N.: Prehistoric earthquake history revealed by lacustrine slump deposits, Geology, 30, 1131–1134, 2002.
Souchère, V., Cerdan, O., Ludwig, B., Le Bissonnais, Y., Couturier, A., and Papy, F.: Modelling ephemeral gully erosion in small cultivated catchments, Catena, 50, 489–505, 2003.
Stewart, M. M., Grosjean, M., Kuglitsch, F. G., Nussbaumer, S. U., and von Gunten, L.: Reconstructions of late Holocene paleofloods and glacier length changes in the Upper Engadine, Switzerland (ca. 1450 BC-AD 420), Palaeogeogr. Palaeocl., 311, 215–223, 2011.
Talbot, M. R. and Livingstone, D. A.: Hydrogen index and carbon isotopes of lacustrine organic matter as lake level indicators, Palaeogeogr. Palaeocl., 70, 121–137, 1989.
Tanasienko, A. A., Yakutina, O. P., and Chumbaev, A. S.: Snowmelt runoff parameters and geochemical migration of elements in the dissected forest-steppe of West Siberia, Catena, 78, 122–128, 2009.
Tanasienko, A. A., Yakutina, O. P., and Chumbaev, A. S.: Effect of snow amount on runoff, soil loss and suspended sediment during periods of snowmelt in southern West Siberia, Catena, 87, 45–51, 2011.
Tropeano, D. and Turconi, L.: Using Historical Documents for Landslide, Debris Flow and Stream Flood Prevention. Applications in Northern Italy, Nat. Hazards, 31, 663–679, 2004.
Tyson, R. V.: Sedimentary Organic Matter: Organic Facies and Palynofacies, Chapman and Hall, London, 615 pp., 1995.
Vannière, B., Wirth, S., Simonneau, A., Gilli, A., Joannin, S., Chapron, E., Anselmetti, F. S., and Magny, M.: Orbital and solar control versus human activities impact on European "Flooding Increase Periods" (the record of Lake Ledro, Northern Italy), Clim. Past, in preparation, 2012.
von Grafenstein, U., Erlenkeuser, H., Brauer, A., Jouzel, J., and Johnsen, S. J.: A Mid-European Decadal Isotope-CLimate Record from 15,500 to 5000 Years B.P., Science, 284, 1654–1657, 1999.
Wanner, H., Solomina, O., Grosjean, M., Ritz, S. P., and Jetel, M.: Struture and origin of Holocene cold events, Quaternary Sci. Rev., 30, 3109–3123, 2011.
Wirth, S. B., Girardclos, S., Rellstab, C., and Anselmetti, F. S.: The sedimentary response to a pioneer geo-engineering project: Tracking the Kander River deviation in the sediments of Lake Thun (Switzerland), Sedimentology, 58: 1737–1761, 2011.

Wirth, S. B., Gilli, A., Glur, L., Anselmetti, F. S., Ariztegui, D., Simonneau, A., Chapron, E., Vannière, B., and Magny, M.: Reconstructing the seasonality of late Holocene flood events using varved lake sediments of Lake Ledro (Southern Alps, Italy), 3rd PAGES Varves Working Group Workshop, Manderscheid, Germany, 2012.

Wohl, E. E.: Inland Flood Hazards: Human, Riparian, and Aquatic Communities, Cambridge University Press, 2000.

Table 1. Historical earthquakes documented by Guidoboni et al. (2007) close to Lake Ledro (http://storing.ingv.it/cfti4med/).

Year	Location	Distance from Lake Ledro	Equivalent magnitude M_e	Epicentral intensity at epicentre I_0
2004 AD	Salo	~ 35 km SSW		VIII
1901 AD	Salo	~ 35 km SSW	5.7	VIII
1891 AD	Illasi valley	~ 55 km SE	5.9	VIII-IX
1117 AD	Verona	~ 53 km SSE	6.8	IX
1046 AD	Adige valley	~ 25 km E	6	IX

Table 2. Estimated ages and characteristics of sedimentary events (SE) interpreted as sub aquatic mass movements triggered in Lake Ledro by regional earthquakes as discussed in the text.

Events	Thickness in core LL082 (cm)	Estimated ages inferred from Vannière et al. (this issue)	Regional earthquakes	Numbers of associated mass wasting deposits	Likelihood of earthquake triggering
SE 1	11.8	2005 AD ± 3	Salo (2004 AD)	2	Very high
SE 2	1.5	AD1871±39	Salo (1901 AD)	?	High
SE 3	1.5	1863 AD ± 42	Illasi valley (1891 AD)	?	High
SE 4	10.8	1044 AD ± 127	Verona (1117 AD) or Adige valley (1046 AD)	9	Very high
SE 5	4.4	1256 ± 115 cal. yr BP		3	High
SE 6	5.3	2545 ± 104 cal. yr BP	Iseo event (2525 ± 110 cal BP)	5	Very high
SE 7	1.6	2595 ± 102 cal. yr BP	Iseo event (2525 ± 110 cal BP)	?	High
SE 8	2.9	3348 ± 79 cal. yr BP		?	Moderate
SE 9	4.6	3815 ± 84 cal. yr BP		2	High
SE 10	1.5	4742 ± 156 cal. yr BP	Iseo event (4488 ± 110 cal BP)	?	High
SE 11	16.1	5889 ± 92 cal. yr BP		10	High
SE 12	13	7190 ± 127 cal. yr BP		10	High
SE 13	5	9183 ± 84 cal. yr BP		2	High
SE 14	4.6	11493 ± 339 cal. yr BP		2	High

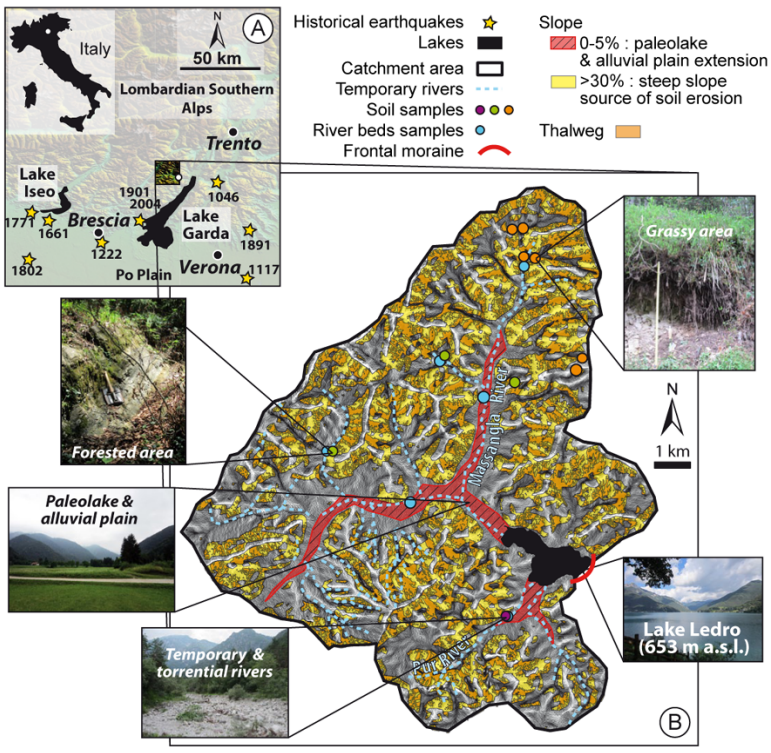

Fig. 1. Location of Lake Ledro in the Italian Alps **(A)** and geomorphological characteristics of its catchment area **(B)**. The Trento area is an active seismic region highlighted by historical earthquakes (yellow stars). Catchment area of Lake Ledro is mainly defined by temporary rivers and steep slopes where soils and rivers samples have been collected.

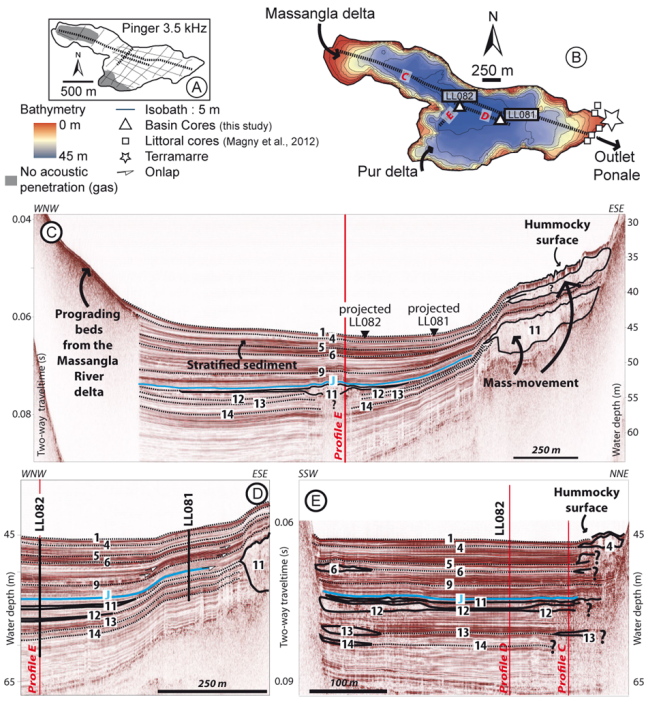

Fig. 2. Seismic stratigraphy of Lake Ledro, based on a dense grid of profiles **(A)**. The bathymetric map is generated from the seismic data **(B)**. Three main profiles: **(C)**, **(D)** and **(E)** are selected to show the different acoustic facies. Numbers 1 to 14 correspond to some light-coloured sedimentary events identified in cores.

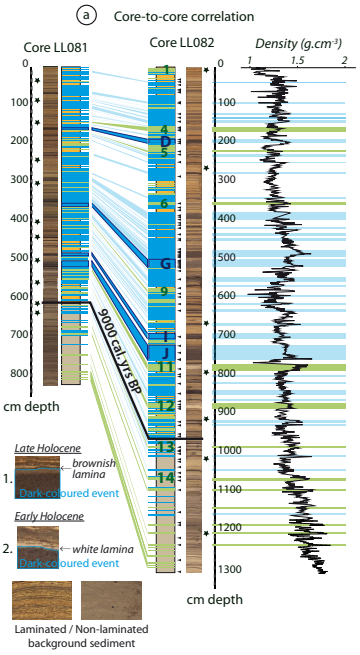

Fig. 3. Core to core correlation between LL081 and LL082 and selected digital photographs of core sections **(a)** illustrating the occurrence of sedimentary events intercalated within the background sedimentation. Black stars are showing the depths of available dates described in Vannière et al (this issue) and black triangles are locating samples analysed by organic geochemistry in this study. A zoom of sediment bulk density profile is given in **(b)** for selected dark-coloured SE (J and D) and in **(c)** for selected light-coloured SE (4 and 12).

Discussion Paper | Discussion Paper | Discussion Paper | Discussion Paper |

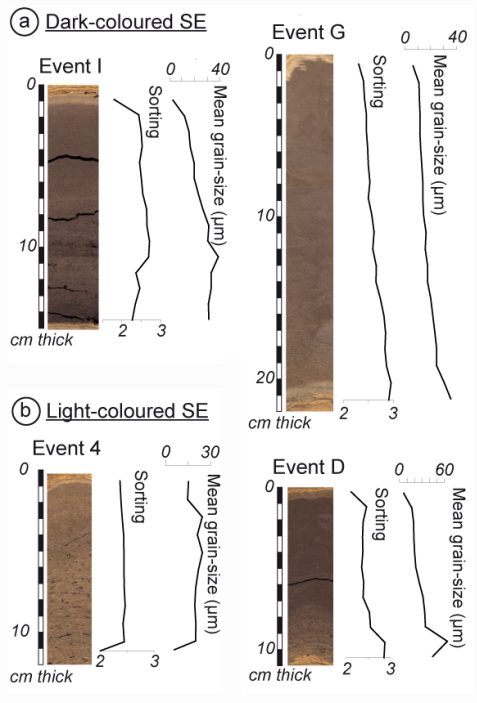

Fig. 4. Grain-size parameters obtained on several dark- and light-coloured deposits from core LL082 (**a** and **b**, respectively).

Discussion Paper | Discussion Paper | Discussion Paper | Discussion Paper |

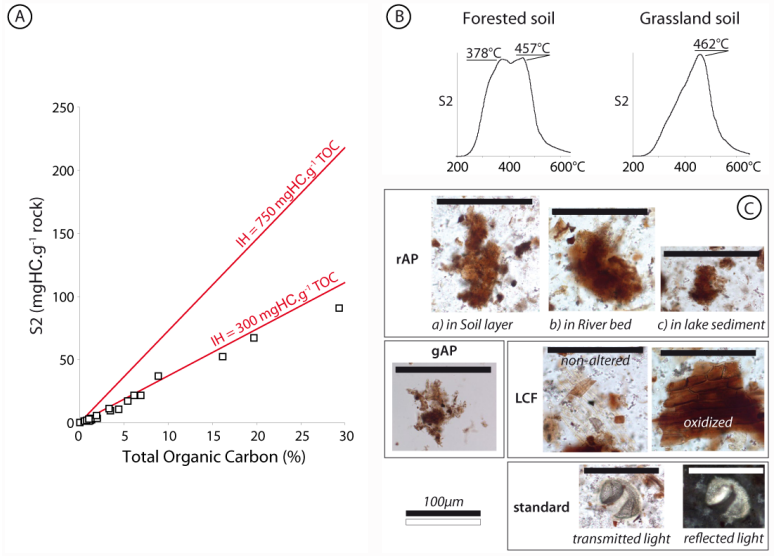

Fig. 5. Rock-Eval results **(A)** of soils and river-beds samples are represented by the diagram S2 *versus* Total Organic Carbon (TOC, %). The two linear domains of Hydrogen Index (HI = 750 and HI = 300 mgHC g^{-1}TOC) corresponding to algal and terrestrial poles, respectively, are represented. S2 curve **(B)** from Rock Eval analysis on superficial layers from forested and grassland soils are also presented. Thermal cracking of the hydrocarbon compounds are represented by the temperature. Organic particles identified by quantitative organic petrography are illustrated in **(C)**: red Amorphous Particles (rAP) in soil layers, river beds and lacustrine sediment; grey Amorphous Particles (gAP); ligno-cellulosic fragments (LCF) non-altered or oxidized; and the standard added in transmitted and reflected light modes.

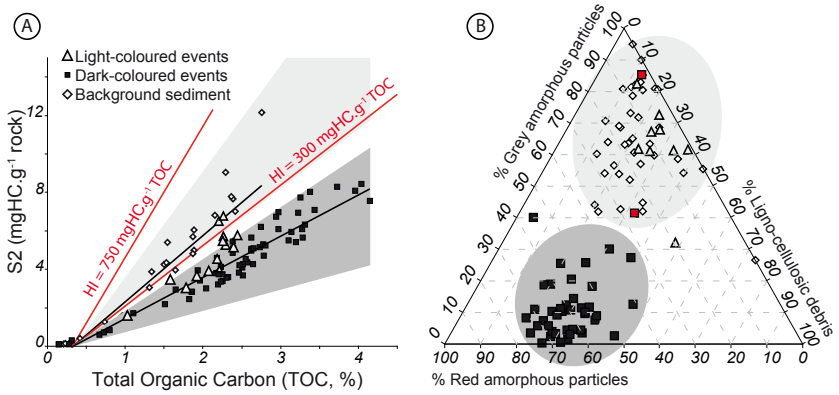

Fig. 6. Organic geochemistry of core LL082. Rock-Eval results **(A)** are represented by the diagram S2 *versus* Total Organic Carbon (TOC, %). Solid lines indicate the regressions line for background sediment samples and dark events samples, respectively. Specific organic signature is given by quantitative organic petrography **(B)** represented on a triangular diagram showing the mass percentage of grey amorphous particles, red ones and ligno-cellulosic debris making up each sample.

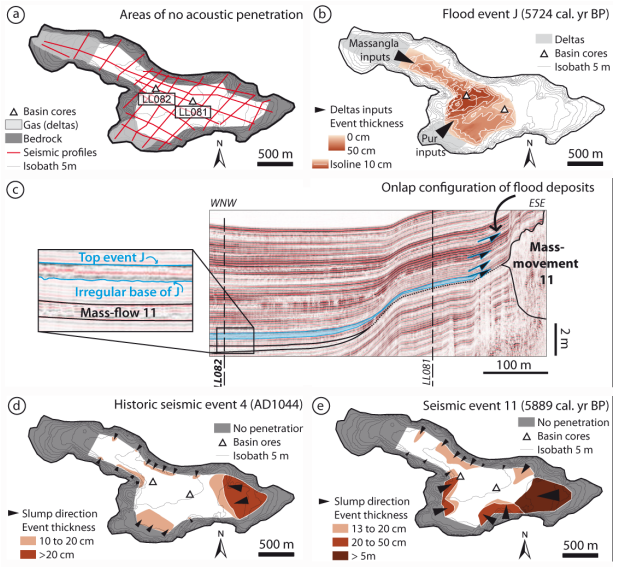

Fig. 7. Grid of 3.5 kHz seismic survey acquired for this study in Lake Ledro and windows of no acoustic penetrations (due to coarse and gas-rich deltaic sediments or bedrock occurrence) are localized **(a)**. **(b)** is illustrating the distribution and thickness of hyperpycnal flood event J characterized by an erosive base and the development of onlap configurations on seismic profiles **(c)**. In **(d)** and **(e)** the distribution and thickness of mass-flow deposits caused by historical earthquakes event 4 and by prehistorical event 11 **(e)** are illustrated and clearly contrasting with the ones of flood event J.

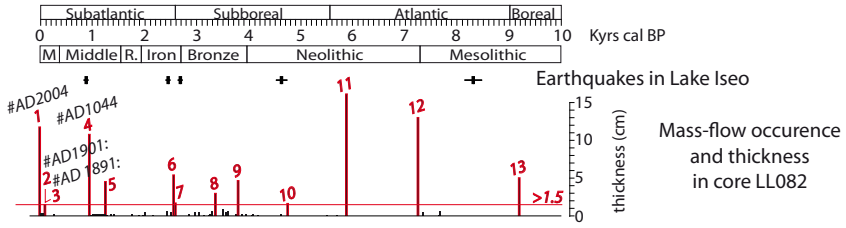

Fig. 8. Illustration of mass-flow occurrence, thickness and age in core LL082. Some mass flow deposits superior to 1.5 cm thick are contemporaneous to historical earthquakes (#) and prehistorical earthquakes (+) documented in nearby Lake Iseo by Lauterbach et al. (2012).

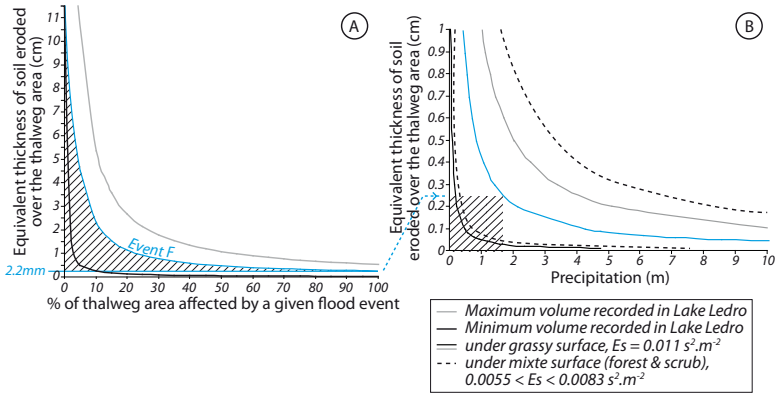

Fig. 9. Illustration of the steps used to estimate the equivalent soil thickness eroded over the catchment area associated with a flood deposit in Lake Ledro **(A)** and the related amount of precipitations when applying the De Ploey et al. (1995) model **(B)**.

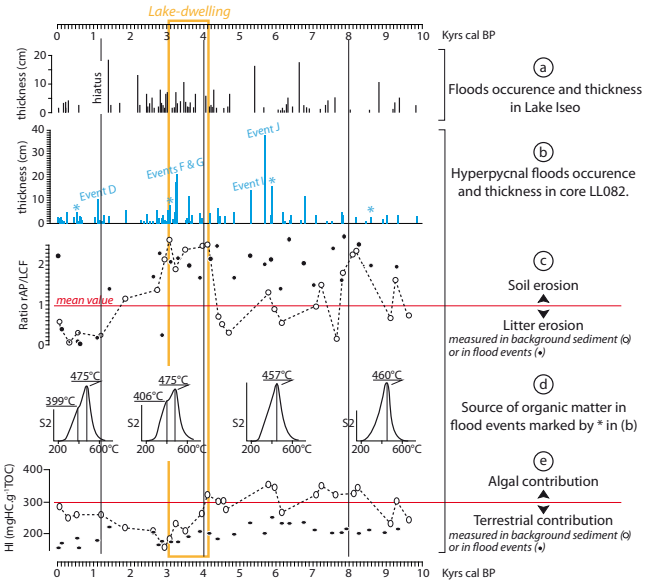

Fig. 10. Chronology and thickness of Holocene hyperpycnal flood events in the Southern Alps documented by Lauterbach et al (2012) in Lake Iseo **(a)**, and higher than 1 cm thick in core LL82 from Lake Ledro **(b)**, the evolution of the source of material remobilized by runoff processes within Lake Ledro watershed is given in **(c)** and calculated by the ratio rAP (red Amorphous Particles) on LCF (Ligno Cellulosic Fragments) for background sediment (white dots) and flood sedimentary events (black dots) in core LL082. The S2 curves from flood deposits (marked by a star in **b**) are given in **(d)** and indicate the type of organic matter present in these events as discussed in the text. The hydrogen index (HI) given in **(e)** is measured in background sediment (white dots) and flood sedimentary events (black dots) from core LL082.